

# Thermal Properties of Low Loss PTFE-CeO<sub>2</sub> Dielectric Ceramic Composites for Microwave Substrate Applications

P. S. Anjana,<sup>1</sup> S. Uma,<sup>2</sup> J. Philip,<sup>2</sup> M. T. Sebastian<sup>1</sup>

<sup>1</sup>Materials and Minerals Division, National Institute for Interdisciplinary Science and Technology (CSIR), Thiruvananthapuram 695019, Kerala, India

<sup>2</sup>Department of Instrumentation & STIC, Cochin University of Science and Technology, Cochin 682022, Kerala, India

Received 28 June 2009; accepted 30 October 2009

DOI 10.1002/app.31690

Published online 26 May 2010 in Wiley InterScience (www.interscience.wiley.com).

**ABSTRACT:** Polytetrafluoroethylene (PTFE) composites filled with CeO<sub>2</sub> were prepared by powder processing technique. The PTFE is used as the matrix and the loading fraction of CeO<sub>2</sub> in the composite varied up to 0.6 volume fraction. The thermal conductivity and coefficient of thermal expansion were studied in relation to filler concentration. The thermal conductivity increased and coefficient of thermal expansion decreased with increase in CeO<sub>2</sub> content. For 0.6 volume fraction loading of the ceramic, the composite has a thermal conductivity of 3.1 W/m°C and

coefficient of thermal expansion 19.6 ppm/°C. Different theoretical approaches have been employed to predict the effective thermal conductivity and coefficient of thermal expansion of composite systems and the results were compared with the experimental data. © 2010 Wiley Periodicals, Inc. *J Appl Polym Sci* 118: 751–758, 2010

**Key words:** composites; dielectric properties; thermogravimetric analysis; differential scanning calorimetry; thermal properties

## INTRODUCTION

The electronic packaging has continuously provided the impetus pushing the development of new materials in a fascinating and rich variety of applications.<sup>1</sup> Thermal considerations in the electronic package have become increasingly important because integration of transistors has resulted in the escalation of power dissipation as well as an increase in heat flux at the devices. Hence the desire for improving thermal properties of materials for electronic component parts is getting stronger and the material performance has become a critical design consideration for packages.<sup>2</sup> Historically, metal components in integrated circuit packages have provided thermal paths for the removal of heat; however, this mechanism has reached its maximum potential. As a result, the polymeric materials in the components are increasingly important as thermal paths for the removal of excess heat that builds up. Unfortunately, polymeric materials are inherently poor thermal conductors, and they must be modified to assist in heat removal from electronics.<sup>3,4</sup>

Fillers play an important role in the production of polymeric materials. In addition to cost saving, other value-added properties are gained through the use of fillers.<sup>5</sup> Fillers can improve the mechanical<sup>6,7</sup> and thermal properties<sup>8–10</sup> as well as optical and electrical properties<sup>11–13</sup> of a polymeric material. Ceramic fillers are often added to polymers to increase the resultant thermal conductivity of the composites.<sup>14</sup> Considerable amount of literature is available on the thermal conductivity of polymers by fillers.<sup>11–13,15</sup> Thermally conductive, electrically insulative, cost effective, and design flexible ceramic particle loaded PTFE composites are increasingly used for electronic packaging and substrate applications.<sup>16</sup> PTFE exhibits useful properties over the widest temperature range of any known polymer. PTFE has a high virgin crystalline melting point (325–335°C), extremely high shear viscosity (10<sup>11</sup> Poise at 380°C) in the melt, good thermal and chemical stability.<sup>17,18</sup> Its combination of electrical properties (relative permittivity ( $\epsilon_r$ ) = 2.1 and dielectric loss ( $\tan \delta$ ) = 10<sup>-5</sup> at 800 MHz) is outstanding with high dielectric strength and extremely low dielectric loss.<sup>19</sup> However, the disadvantages of PTFE substrate include low thermal conductivity (0.26 W/m°C),<sup>17</sup> high linear coefficient of thermal expansion (>100 ppm/°C) and low surface energy.<sup>20,21</sup> Addition of metallic fillers, although have high thermal conductivity adversely affect the dielectric properties of the composites. Hence ceramics having low thermal expansion coefficient, high thermal conductivity along with low dielectric

Correspondence to: M. T. Sebastian (mailadils@yahoo.com).

Contract grant sponsors: Council of Scientific and Industrial Research and Department of Science and Technology, New Delhi.

loss are preferred as fillers. A substantial amount of work has been reported to modify the dielectric and thermal properties of various polymer-ceramic composites for packaging applications.<sup>22-24</sup> Price et al.<sup>17</sup> reported the thermal conductivity of PTFE and PTFE composites. Chen et al.<sup>20</sup> reported the effect of SiO<sub>2</sub> filler content and size on the dielectric and thermal properties of PTFE. Ceria possess good dielectric and thermal properties. It has a relative permittivity of 23, dielectric loss of 0.00001 at 7 GHz, thermal conductivity of 12 W/m°C and thermal expansion coefficient of 12.58 ppm/°C.<sup>25-27</sup> Anjana et al.<sup>25</sup> reported that PTFE-CeO<sub>2</sub> composites possess good microwave dielectric properties useful for microwave substrate applications. The present article investigates the thermo-physical properties of PTFE-CeO<sub>2</sub> composites at room temperature for the first time to understand the thermal stability and heat transport performance. The article also discusses the comparison of experimental results with theoretical predictions from well-known models in literature.

## EXPERIMENTAL

### Materials and methods

CeO<sub>2</sub> (99.9%, Indian Rare Earth, Udyogamandal, India) - PTFE (Hindustan Fluorocarbons, Hyderabad, India) composites were prepared by powder processing technology. To create an active surface for binding with polymer, the fine powder of CeO<sub>2</sub> was mixed with acrylic acid solution for 1 h and dried.<sup>10</sup> Acrylic acid is a well-known polymerizing agent. The dried powder was again treated with 2 wt % tetra butyl titanate. The use of titanate based coupling agents provides excellent mechanical and electrical properties compared to other organic functional coupling agents like silane. The evaporation of the solvent gives CeO<sub>2</sub> powders, clad with coupling agents. Different volume fractions (0-0.6) of treated ceramics and PTFE powders were dispersed in ethyl alcohol using ultrasonic mixer for about 30 min. A dried powder mixture was obtained by removing the solvent at 70°C under stirring. The homogeneously mixed PTFE-CeO<sub>2</sub> powders were then hot-pressed under uniaxial pressure of 50 MPa at 330°C for 15 min and then slowly cooled to room temperature.

### Characterization

The density of the composites ( $\rho$ ) was determined using Archimedes method. The composites were characterized by X-ray diffraction technique using CuK $\alpha$  radiation (Philips X-Ray Diffractometer). The surface morphology of the composites was studied by scanning electron microscope (JEOL-JSM 5600 LV, Tokyo, Japan).

The DSC analysis was done by Perkin Elmer DSC 7. The instrument was computer controlled and calculations were done using Pyris software. 5-10 mg of samples were sealed in aluminum pans and heated from 25°C to 600°C at rate of 5°C/min and cooled to 25°C at the same rate.

Photopyroelectric technique<sup>28,29</sup> was used to determine the thermal conductivity of the PTFE-CeO<sub>2</sub> composites. A 70 mW He-Cd laser of wavelength 442 nm, intensity modulated by a mechanical chopper (Stanford Research Systems Model SR 540) was used as the optical heating source. A PVDF film of thickness 28  $\mu$ m, with Ni-Cr coating on both sides, was used as the pyroelectric detector. The output signal was measured with a lock-in amplifier (Stanford Research Systems Model SR 830). Modulation frequency was kept above 60 Hz to ensure that the detector, the sample and backing medium are thermally thick during measurements. The thermal thickness of the composites was verified by plotting photopyroelectric (PPE) amplitude and phase with frequency at room temperature. Thermal diffusivity ( $\alpha$ ) and thermal effusivity ( $e$ ) were also measured from PPE signal phase and amplitude.<sup>30</sup> From the values of  $\alpha$  and  $e$ , the thermal conductivity and specific heat capacity of the samples were obtained.

Heat treated cylindrical samples of dimensions (diameter = 8 mm and height = 10 mm) were used to measure the coefficient of thermal expansion (CTE) of the PTFE-CeO<sub>2</sub> composites using a thermo-mechanical analyzer (Shimadzu Model TMA-60 H), in the temperature 25-270°C.

The micromechanical properties of PTFE-CeO<sub>2</sub> composites were measured using micro hardness tester (Clemex Model 4). Both the surfaces of the samples were polished to have optically flat surface for indentation. The specimen was subjected to a load of 50 g and dwell time of 10 s. For pure ceramic sample the load was increased to 400 g. A total of 10 readings were taken to get the average hardness.

### Theoretical modeling

#### Thermal conductivity

Determining the thermal conductivity of composite materials is crucial in a number of industrial processes. The effective thermal conductivity of a heterogeneous material is strongly affected by its composition, crystal structure, distribution within the medium, and contact between the particles. Numerous theoretical and experimental approaches have been developed to determine the precise value of thermal conductivity. Comprehensive review articles have discussed the applicability of several models that appear to be more promising.<sup>31-33</sup>

For a two-component composite, the simplest model would be with the materials arranged in either parallel or series with respect to heat flow, which gives the upper or lower bounds (also referred to as Weiner bounds) of effective thermal conductivity.<sup>34</sup> In this study, following models were used to calculate the effective thermal conductivity of PTFE composites:

*Geometric Mean Model:*

$$k_c = k_f^{V_f} k_m^{1-V_f} \tag{1}$$

where  $k_c$ ,  $k_f$ , and  $k_m$  are the thermal conductivities of composite, filler, and matrix, respectively and  $V_f$  is the volume fraction of the filler in the PTFE-CeO<sub>2</sub> composite.

*Effective-Medium Theory (EMT) Model.* The Effective-medium theory (EMT) assumes that the composite system is a homogeneous medium and the EMT equation for thermal conductivity can be derived through the Laplace equation for thermal transfer, which can be expressed as<sup>34,35</sup>

$$V_m \frac{k_m - k_c}{k_m + 2k_c} + V_f \frac{k_f - k_c}{k_f + 2k_c} = 0 \tag{2}$$

where  $V_m$  is the volume fraction of PTFE in the PTFE-CeO<sub>2</sub> composite and  $k_c$ ,  $k_f$ ,  $k_m$ ,  $V_f$  same as in eq. (1).

*Cheng-Vachon Model.* Based on Tsao's model, which gives the thermal conductivity of two phase solid mixture,<sup>36</sup> Cheng and Vachon assumed a parabolic distribution of the discontinuous phase in the continuous phase. The constants of this parabolic distribution were determined by analysis and presented as a function of the discontinuous phase volume fraction. Thus, the equivalent thermal conductivity of the two phase solid mixture was derived in terms of the distribution function, and the thermal conductivity of the constituents. For  $k_f > k_m$ ,

$$\frac{1}{k_c} = \frac{1}{\sqrt{C(k_f - k_m)[k_m + B(k_f - k_m)]}} \times \ln \frac{\sqrt{[k_m + B(k_f - k_m)]} + \frac{B}{2} \sqrt{C(k_f - k_m)}}{\sqrt{[k_m + B(k_f - k_m)]} - \frac{B}{2} \sqrt{C(k_f - k_m)}} + \frac{1 - B}{k_m} \tag{3}$$

where

$$B = \sqrt{3V_f/2} \quad C = -4\sqrt{2/3V_f}$$

Coefficient of thermal expansion (CTE)

Thermal expansion coefficients of composites are very important in relation to the dimensional stability and the mechanical compatibility when used with other materials. A considerable amount of work has

been done to predict the thermal expansion coefficients of composites.<sup>37-39</sup> The rule of mixtures serves as the first order approximation to the overall calculation of the coefficient of thermal expansion of the composite.<sup>40</sup> This can be expressed as

$$\alpha_c = V_f \alpha_f + (1 - V_f) \alpha_m \tag{4}$$

where  $\alpha_c$ ,  $\alpha_m$ , and  $\alpha_f$  are coefficient of thermal expansion of the composite, matrix, and filler, respectively. Turner developed a model that takes into account the mechanical interaction between different materials in the composite.<sup>41</sup> Based on the assumption that all phases in the composite have the same dimension change with temperature, he derived a relationship, which is expressed as

$$\alpha_c = \frac{(1 - V_f)B_m \alpha_m + V_f B_f \alpha_f}{(1 - V_f)B_m + V_f B_f} \tag{5}$$

where  $B_f$ ,  $B_m$  are Bulk Modulus of filler and matrix, respectively. Schapery developed a model to predict the upper and lower bounds of the CTE of a composite.<sup>42</sup> The two bounds are given by

$$\alpha_c^l = \alpha_m + \frac{B_f (B_m - B_c^u) (\alpha_f - \alpha_m)}{B_c^u (B_m - B_f)} \tag{6}$$

$$\alpha_c^u = \alpha_m + \frac{B_f (B_m - B_c^l) (\alpha_f - \alpha_m)}{B_c^l (B_m - B_f)} \tag{7}$$

where subscript "u" and "l" refer to the upper and lower bounds, respectively. It can be seen that the upper and lower bounds as calculated from the Hashin-Shtrikman model are used to calculate the lower and upper bounds in the Schapery model. Hashin and Shtrikman model<sup>43</sup> assumes a homogeneous and isotropic reference material, in which the constituents are dispersed. Depending on whether the stiffness of the reference material is more or less than that of the reinforcement, the lower and upper bounds are calculated as:

$$B_c^u = B_f + \frac{1 - V_f}{\frac{1}{B_m - B_f} + \frac{3V_f}{(3B_f + 4G_f)}} \tag{8}$$

$$B_c^l = B_m + \frac{V_f}{\frac{1}{B_f - B_m} + \frac{3(1 - V_f)}{(3B_m + 4G_m)}} \tag{9}$$

where  $G_f$  and  $G_m$  represents the Shear Modulus of filler and PTFE, respectively.

## RESULTS AND DISCUSSION

The density of a two-component mixture should depend on the densities of the constituent

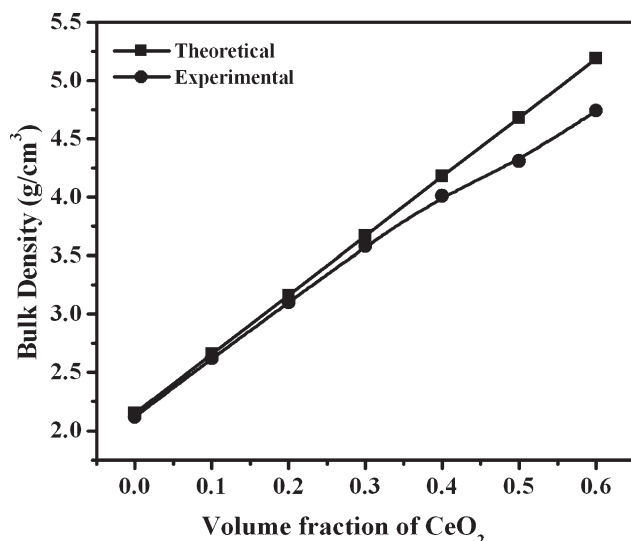


**Figure 1** Variation of density with volume fraction in PTFE-CeO<sub>2</sub> composites.

components and also on their proportion by weight. Figure 1. depicts the measured and theoretical densities of PTFE-CeO<sub>2</sub> composites as a function of volume fraction. The density is measured using Archimedes method and compared with the mixing rule<sup>44</sup>

$$\rho_{eff} = V_f \rho_f + V_m \rho_m \quad (10)$$

where  $\rho_{eff}$ ,  $\rho_f$ ,  $\rho_m$  are the densities of composite, filler, and matrix, respectively. The experimental values for lower volume fractions agree well with the theoretical values. The measured density increases with filler content due to the higher density of CeO<sub>2</sub>. The deviation of measured density from theoretical values increases with the filler content. The relative density decreases from 98.6% for 0.1  $V_f$  to 91.4% for 0.6  $V_f$  (Table I). This may be due to the increase in void formation inside the composite for higher filler content.

Figure 2(a)-(b) shows the X-ray diffraction of PTFE and 0.3 volume fraction ( $V_f$ ) PTFE-CeO<sub>2</sub> composite. The pattern of PTFE shows a strong crystalline peak (at  $2\theta = 18^\circ$ ), superimposed over an amorphous halo as reported.<sup>45</sup> XRD profile of 0.3  $V_f$  of PTFE-CeO<sub>2</sub> composite shows that there are no undesired secondary phases [Fig. 2(b)]. The XRD peaks corresponding to CeO<sub>2</sub> are indexed based on JCPDS file no. 34-0394.

Figure 3 shows the SEM pictures of PTFE-CeO<sub>2</sub> composites with different volume fractions. The CeO<sub>2</sub> particles are randomly distributed throughout the PTFE matrix. For higher volume fractions of the composites, there is aggregation of CeO<sub>2</sub> particles. With the increase of filler content, the packing of particles grew denser [Fig. 3(b,c)]. These results indicated the excellent compatibility between PTFE and CeO<sub>2</sub> particles. CeO<sub>2</sub> powder used in the present study is having approximately 5–10  $\mu\text{m}$  [Fig. 3(d)].

Table I gives the relative permittivity and dielectric loss of PTFE-CeO<sub>2</sub> composites at 7 GHz. The relative permittivity and dielectric loss increase as the volume fraction of filler (CeO<sub>2</sub>) increases from 0.1 to 0.6. The increase in relative permittivity is expected as the CeO<sub>2</sub> ceramic has a higher relative permittivity compared to that of PTFE matrix. The dielectric loss, which is the main factor affecting the frequency selectivity of a material is influenced by many factors, such as porosity, microstructure, and defects.<sup>25</sup> The coefficient of temperature variation of relative permittivity ( $\tau_\epsilon$ ) depends on the thermal expansion coefficient of the composite according to the relation

$$\tau_f = -\alpha_c - \frac{\tau_\epsilon}{2} \quad (11)$$

where  $\tau_f$  is the coefficient of temperature variation of resonant frequency and  $\alpha_c$  is the coefficient of thermal expansion of the composite.

**TABLE I**  
The Relative Density, Dielectric Properties (at 7 GHz) and Summary of Data Obtained via the TGA and DSC Measurements for Virgin PTFE and PTFE-CeO<sub>2</sub> Composites

Composition of PTFE-CeO <sub>2</sub>	Relative density (%)	$\epsilon_r$ (at 7 GHz)	$\tan \delta$ (at 7 GHz)	CeO <sub>2</sub> content <sup>a</sup> $W_f^a$	CeO <sub>2</sub> content <sup>b</sup> $W_f^b$	$T_d$ (°C)	$T_t$ (°C)	$T_m$ (°C)	$T_o$ (°C)	$T_c$ (°C)
100-0	98.6	1.95	0.0008	0.0	0.0	529	20.1	328.5	316.2	312.5
90-10	98.4	2.13	0.0022	27.0	25.0	528	19.2	326.4	317.4	313.7
80-20	98.1	2.33	0.0031	45.6	44.8	530	19.8	327.2	316.8	312.8
70-30	97.5	2.73	0.0043	59.0	59.0	529	19.9	327.3	316.7	312.5
60-40	95.9	3.87	0.0047	69.0	68.5	528	19.6	327.5	317.1	313.3
50-50	92.3	4.14	0.0058	77.0	76.0	530	19.5	326.5	316.7	312.6
40-60	91.4	4.99	0.0064	83.0	80.0	527	19.0	326.2	316.9	312.1

$T_d$  is the temperature at which 10 wt % of the sample is lost after heating in nitrogen atmosphere by TGA,  $T_t$  is the first order transition temperature,  $T_m$  is the melting temperature,  $T_c$  is the temperature of crystallization,  $T_o$  is the onset crystallization temperature.  $W_f^a$  is the weight fraction of CeO<sub>2</sub> content in the PTFE-CeO<sub>2</sub> composite,  $W_f^b$  is the weight fraction of CeO<sub>2</sub> content in the PTFE-CeO<sub>2</sub> composite by TGA.

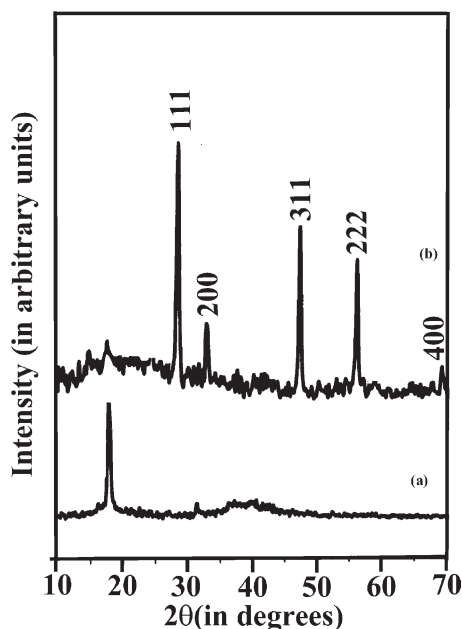


**Figure 2** XRD patterns of (a) PTFE (b) 0.3  $V_f$  of PTFE-CeO<sub>2</sub> composites.

The TGA measurements of PTFE-CeO<sub>2</sub> composites as shown in Figure 4 show that the heat resistance of PTFE is very good. The polymer begins to decompose around 530°C and a residue is observed at 600°C, which corresponds to the CeO<sub>2</sub> content. Table I lists the decomposition temperature ( $T_d$ ) of PTFE-CeO<sub>2</sub> composites for different filler contents of CeO<sub>2</sub>. It shows that the total mass loss values are in

good agreement with the amount of CeO<sub>2</sub> originally mixed into the different volume fractions of PTFE-CeO<sub>2</sub> samples and the decomposition temperature was not affected by the CeO<sub>2</sub> content. This is due to the highly unreactive nature of PTFE matrix with CeO<sub>2</sub>.

A typical DSC thermogram of 0.3  $V_f$  CeO<sub>2</sub> loaded PTFE is shown in Fig. 5, in which two peaks appear at 19.9°C and 327.3°C, respectively, in the heating mode. The melting point of PTFE is around 325–330°C and it has several first or second order transition temperatures ranging from –110 to 140°C.<sup>20</sup> PTFE shows low temperature phase transitions at about 19 and 30°C at atmospheric pressure.<sup>46</sup> The crystal structure of PTFE is triclinic at temperatures below 19°C and above that temperature the unit cell changes to hexagonal. The three-dimensional register of chain segments gets lost in the temperature range of 19–30°C and the preferred crystallographic orientation disappears.<sup>47</sup> Therefore, the result suggests that the CeO<sub>2</sub> filled PTFE composites absorb heat to change the crystal formation at 19.9°C and melt at 327.3°C.<sup>48</sup> The sample also get recrystallized by cooling from the molten state so as to observe the crystallization temperature  $T_c$ . The crystallization behavior of materials is characterized using crystallization temperature,  $T_c$  and the onset crystallization temperature,  $T_o$ . Filler induced changes in  $T_t$ ,  $T_m$ ,  $T_o$ , and  $T_c$  of virgin PTFE and PTFE-CeO<sub>2</sub> composites are determined using DSC in the temperature range 0–350°C (Table I). Both endothermic and exothermic curves

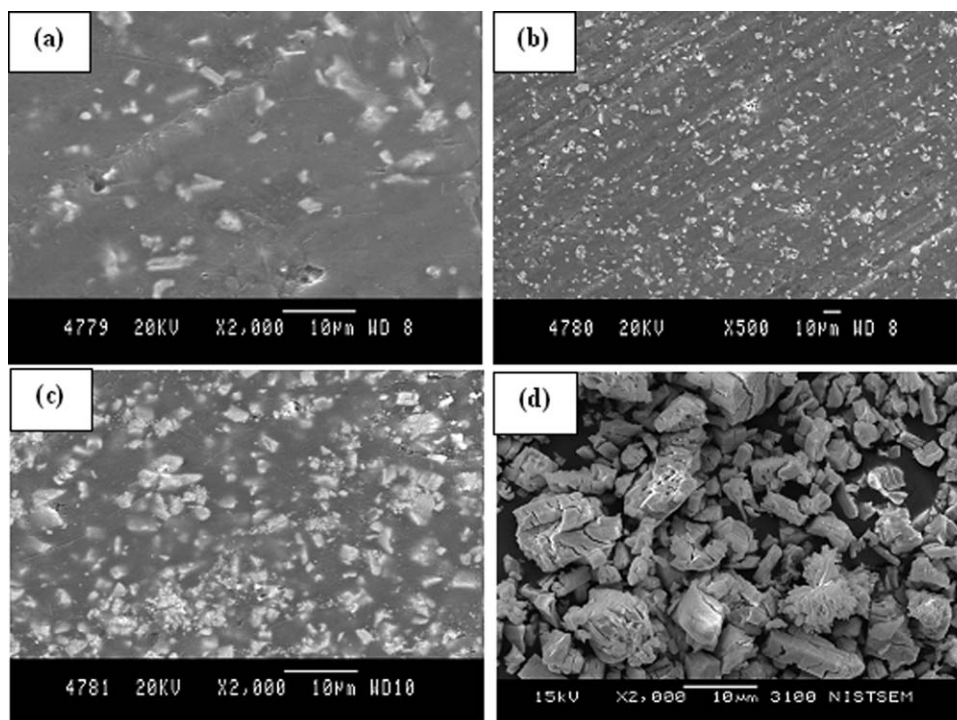


**Figure 3** SEM micrographs of (a) 0.1  $V_f$ , (b) 0.3  $V_f$ , (c) 0.6  $V_f$  of PTFE-CeO<sub>2</sub> composites, and (d) CeO<sub>2</sub> powder.

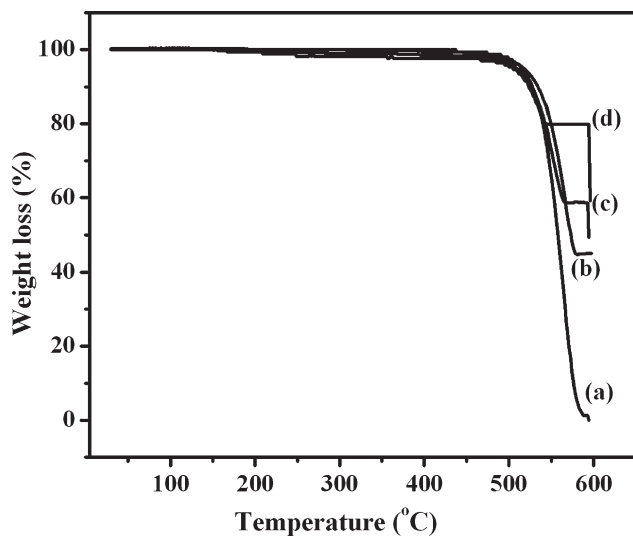


**Figure 4** TGA curves of (a) virgin PTFE, (b) 0.2  $V_f$ , (c) 0.3  $V_f$  and (d) 0.6  $V_f$  of PTFE-CeO<sub>2</sub> composites.

of PTFE-CeO<sub>2</sub> composites are similar to those of pure PTFE.  $T_i$ ,  $T_m$ ,  $T_o$ , and  $T_c$  of the PTFE-CeO<sub>2</sub> composites are very similar to those of pure PTFE, which implies that the existence of the CeO<sub>2</sub> filler has no effect on the melting and crystallization behavior of PTFE.

Figure 6 shows comparison of experimental and predicted values of thermal conductivities using eqs. (1)–(3) of PTFE-CeO<sub>2</sub> composites with varying filler contents. Thermal conductivity increases gradually with CeO<sub>2</sub> filler loading due to the higher thermal conductivity of CeO<sub>2</sub> (12 W/m°C). Thermal conductivity is increased to 3.1 W/m°C (standard deviation  $\pm$  0.01 W/m°C) for 0.6  $V_f$  from 0.26 W/m°C for pure PTFE. A similar observation was reported by Kim et al.<sup>48</sup> in AlN-epoxy composites for 0.6  $V_f$  of AlN. Experimental results are close to the predic-

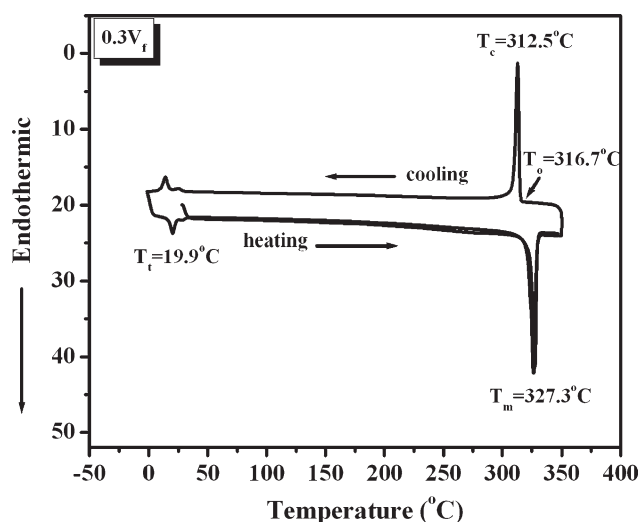


**Figure 5** Heating and cooling DSC curves of the 0.3  $V_f$  CeO<sub>2</sub> reinforced PTFE composite.

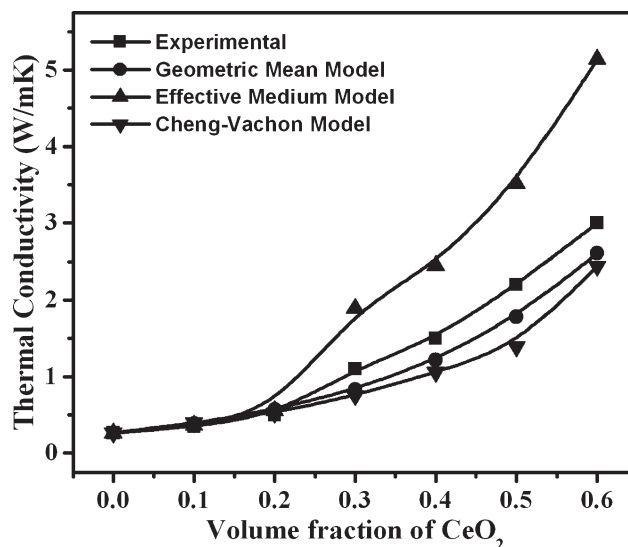


**Figure 6** Experimental and predicted thermal conductivities of PTFE-CeO<sub>2</sub> composites.

tions of Geometric Mean Model and Chen–Vachon Model. As the volume fraction of the filler increases, the mismatch between the matrix and the filler in the form of interfacial gap becomes serious, which is bad for heat conduction.<sup>15</sup> Generally, all theoretical predictions are valid for low filler contents.<sup>15,49</sup> Agari et al.<sup>50</sup> reported that in thermal conduction systems containing a high volume of fillers, particles interact with each other and affect the position of particles in a composite. Hence it is considered that the powder properties of particles (the ease of forming an aggregate of particles, limit of packing, etc.) greatly affect the thermal conductivity of the composite. Theoretical models account for variations in the size, shape, intrinsic thermal conductivity, and state of dispersion of the filler. The wide variation in filler geometry, orientation, and dispersion makes it difficult to compare composites filled with different compounds. Moreover, the interfacial boundary, thermal resistance between the filler particles and the matrix referred to as Kapitza resistance<sup>51</sup> is not taken into account while calculating the thermal conductivity of PTFE-CeO<sub>2</sub> composites. It is not possible to measure it on the molecular level where it takes place.<sup>52</sup> As a result, the experimental and theoretical thermal conductivity data are often not in agreement.<sup>53</sup>

Figure 7 shows the comparison between the experimental data and theoretical models for coefficient of thermal expansion (CTE) of PTFE-CeO<sub>2</sub> composites with varying filler fractions. The CTE decreases with the increasing amount of CeO<sub>2</sub> contents. CeO<sub>2</sub> has CTE of 12.58 ppm/°C (Standard deviation, 0.04 ppm/°C) in the temperature range 25 to 270°C. If a composite is heated, the polymer matrix will expand more than the ceramic fillers. However, if the inter-

phases are capable of transmitting stresses the expansion of the matrix will get reduced.<sup>54</sup> CTE is decreased to 19.6 ppm/°C from 99.3 ppm/°C (for PTFE) for a filler loading of 0.6  $V_f$ . The parameters used for the prediction of CTE are  $\alpha_m = 99.3$  ppm/°C,  $\alpha_f = 12.58$  ppm/°C,  $B_f = 220$  GPa,  $B_m = 0.4$  GPa,  $K_f = 149$  GPa, and  $K_m = 0.55$  GPa. The CTE values calculated using rule of mixtures [eq. (4)] are slightly higher than the corresponding experimental values. This may be due to difference in microstructure, bulk modulus, and thermal softening of the components in the composites, which are not accounted in this relation.<sup>24</sup> The values of CTE calculated using Turner equation [eq. (5)] also shows a large deviation from the experimental values. It can be seen that for all volume fractions, the CTE obtained lies in between Schapery's upper and lower bounds [eq. (6), (7)]. The deviation from experimental data is smaller for Schapery's upper bound than the lower bounds. Similar variation of CTE is reported by Wong et al.<sup>41</sup> while calculating the CTE values for epoxy resins filled with silica, alumina, and aluminum nitride.

Micro indentation with a point indenter involving a deformation on a very small scale is one of the simplest ways to measure the mechanical properties of a polymer composite. Micro hardness determination using the imaging method is a promising technique for the morphology-mechanical property correlations in heterophase systems of known composition.<sup>55</sup> It is worth to note from the optical micrographs of the composites that CeO<sub>2</sub> particles are well dispersed in the PTFE matrix. Figure 8 shows the variation of micro hardness with CeO<sub>2</sub> filler loading in PTFE-CeO<sub>2</sub> composites. Vickers microhardness tests are performed for a range of indentation diagonals. Micro hardness of 700 kg/mm<sup>2</sup> is

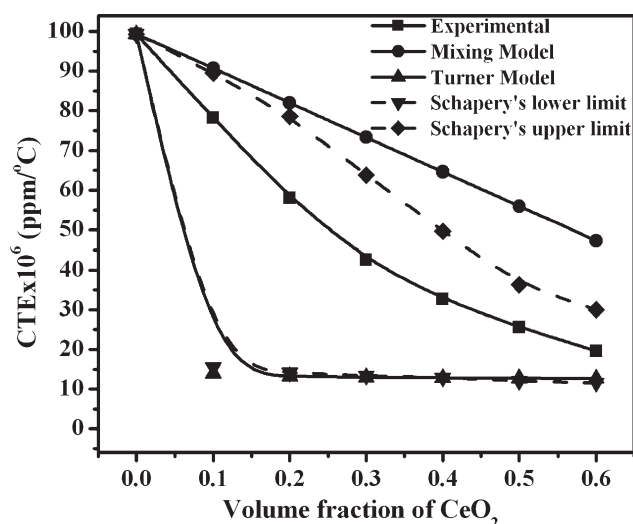


**Figure 7** Experimental and predicted thermal expansion coefficients of PTFE-CeO<sub>2</sub> composites.

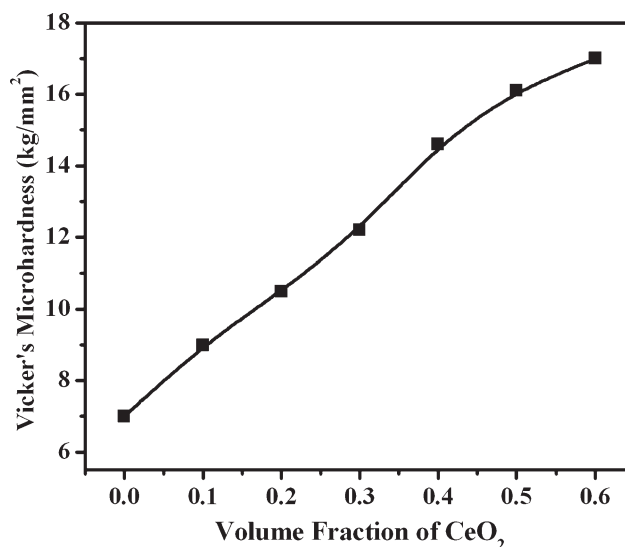


**Figure 8** Variation of Vickers micro hardness with CeO<sub>2</sub> loading in PTFE-CeO<sub>2</sub> composites.

obtained for the sintered and dense CeO<sub>2</sub> for a load of 400g. Virgin PTFE has an average Vickers's hardness of 7 kg/mm<sup>2</sup> and as the volume fraction of CeO<sub>2</sub> loading increases, the hardness also increases in PTFE-CeO<sub>2</sub> composites. An increase in hardness to 17 kg/mm<sup>2</sup> (around 60% increase) is obtained for 0.6  $V_f$ .

## CONCLUSIONS

The PTFE-CeO<sub>2</sub> composites for microwave substrate application are prepared by the powder processing technique. SEM micrographs show that with the increase of filler content, the packing of ceramic particles became denser and indicated the excellent compatibility between PTFE and CeO<sub>2</sub> particles. Thermo gravimetric analysis of PTFE-CeO<sub>2</sub> composites indicates that there is no change in decomposition temperature of PTFE with CeO<sub>2</sub> loading. Differential Scanning Calorimetry analysis indicates that first order transition, melting, onset crystallization, and crystallization temperature of the PTFE-CeO<sub>2</sub> composites are very similar to those of pure PTFE. This implies that the existence of the CeO<sub>2</sub> filler has no effect on the crystallization behavior of PTFE. The thermal conductivity and coefficient of thermal expansion are studied in relation to filler concentration. The thermal conductivity increased and coefficient of thermal expansion decreased with increase in CeO<sub>2</sub> content. For 0.6 volume fraction loading of the ceramic, the composite has thermal conductivity of 3.1 W/m°C and coefficient of thermal expansion 19.6 ppm/°C. The data of thermal conductivity and coefficient of thermal expansion obtained are compared with theoretical models that are used to predict the properties of two phase mixtures. An

increase in Vicker's micro hardness to 17 kg/mm<sup>2</sup> from 7 kg/mm<sup>2</sup> (around 60% increase) is obtained for 0.6  $V_f$  in PTFE- CeO<sub>2</sub> composites.

## References

- Prou, A. Progress in Electromagnetics Research: Dielectric Properties of Heterogeneous Materials; Elsevier: New York, 1992.
- Tummala, R. R.; Rymaszewski, E. J. Microelectronics Packaging Handbook; van Nostrand Reinhold: New York, 1989.
- Procter, P.; Sole, J. Proceedings of 41<sup>st</sup> Electronic and Components Technology Conference; Institute of Electrical and Electronic Engineers: Atlanta, GA, 1991.
- Bujard, P.; Kuhnlein, G.; Ine, S.; Sclobara, T. IEEE Trans Compon Packag Manuf Technol A 1994, 17, 527.
- Luyt, A. S.; Molefi, J. A.; Krump, H. Polym Degrad Stab 2006, 91, 1629.
- Bare, W.; Albano, C.; Reyes, J.; Dominguez, N. Surf Coat Technol 2002, 404, 158.
- Fan, L.; Dang, Z.; Nan, C.-W.; Li, M. Electrochim Acta 2002, 48, 205.
- Korab, J.; Stefanik, P.; Kavecky, S.; Sebo, P.; Korb, G. Compos A Appl Sci Manuf 2002, 33, 577.
- Bigg, D. B. Adv Polym Sci 1995, 119, 1.
- Kim, Y. D.; Oh, N. L.; Oh, S.-T.; Moon, I.-H. Mater Lett 2001, 51, 420.
- Yang, L.; Schruben, D. L. Polym Eng Sci 1994, 34, 1109.
- Mamunya, Y. P.; Zois, H.; Apekis, L.; Lebedev, E. V. Powder Technol 2004, 140, 49.
- Balta Calleja, F. J.; Ezquerra, T. A.; Rueda, D. R.; Alonso-Lopez, J. J Mater Sci Lett 1984, 3, 165.
- Bigg, D. M. Polym Compos 1986, 7, 125.
- He, H.; Fu, R.; Han, Y.; Shen, Y.; Song, X. J Mater Sci 2007, 42, 6749.
- Huang, S. L.; Chen, T.-H.; Chen, H. J Reinf Plast Compos 2006, 25, 1053.
- Price, D. M.; Jarralt, M. Thermochim Acta 2002, 392, 231.
- Xiang, F.; Wang, H.; Yao, X. J Eur Ceram Soc 2006, 26, 1999.
- Bur, J. A. Polymer 1985, 26, 963.
- Chen, Y.-C.; Lin, H.-C.; Lee, Y.-D. J Polym Res 2003, 10, 247.
- Arthur, D. J.; Sweig, G. S. U.S. Pat. 149,590 (1992).
- Wang, Y. M.; Jia, D. C.; Zhou, Y. J Polym Res 2003, 10, 247.
- Lu, X.; Xu, G. J Appl Polym Sci 1997, 65, 2733.
- Subodh, G.; Manjusha, M. V.; Philip, J.; Sebastian, M. T. J Appl Polym Sci 2008, 108, 1716.
- Anjana, P. S.; Suma, M. N.; Mohanan, P.; Sebastian, M. T. Int J Appl Ceram Technol 2008, 5, 325.
- Santha, N.; Sebastian, M. T.; Mohanan, P.; Alford, N. Mc. N.; Sarma, K.; Pullar, R. C.; Kamba, A.; Pashkin, P.; Petzelt, J. J Am Ceram Soc 2004, 87, 1233.
- Osaka, M.; Miwa, S.; Tachi, Y. Ceram Int 2006, 32, 659.
- Menon, C. P.; Philip, J. Meas Sci Technol 2000, 11, 1744.
- Marinelli, M.; Murtas, F.; Mecozzi, M. G.; Martellucci, S. Appl Phys A: Mater Sci Process 1990, 51, 387.
- Sebastian, M. T.; Menon, C. P.; Philip, J.; Schwartz, R. W. J Appl Phys 2003, 94, 3206.
- Progelhof, R. C.; Throne, J. L.; Reutsch, R. R. Polym Eng Sci 1976, 16, 615.
- Carson, J. K.; Lovatt, S. J.; Tanner, D. J.; Cleland, A. C. J Food Eng 2006, 75, 297.
- Ott, H. J. Plastic Rubber Process Appl 1981, 1, 9.
- Wang, J.; Carson, J. K.; North, M. F.; Cleland, D. J. Int J Heat Mass Transfer 2006, 49, 3075.
- Maxwell, J. C. A Treatise on Electricity and Magnetism; Dover: New York, 1954.
- Tsao, T. N. G. Ind Eng Chem 1961, 53, 395.
- Kerner, E. H. Proc Phys Soc 1956, 69, 808.
- Wakashima, A.; Otsuka, M.; Umekawa, S. J Compos Mater 1974, 8, 391.
- Ishikawa, T.; Koyama, K.; Kobayashi, S. J Compos Mater 1978, 12, 153.
- Orrhede, M.; Tolani, R.; Salama, K. Res Nondestr Eval 1996, 8, 23.
- Wong, C. P.; Bollampally, R. S. J Appl Polym Sci 1999, 74, 3396.
- Schapery, R. A. J Comp Mater 1968, 2, 380.
- Hashin, Z.; Shtrikman, S. J Mech Phys Solids 1963, 11, 127.
- Grewe, M. G.; Gururaja, T. R.; Shrout, T. R.; Newnham, R. E. IEEE Trans Ultrason Ferroelectrics Freq control 1990, 7, 506.
- Rae, P. J.; Datebaum, B. M. Polymer 2004, 45, 7615.
- Androsch, A.; Wunderlich, B.; Radusch, H. J. J Therm Anal Calorim 2005, 79, 615.
- Endo, M.; Yamada, K.; Tadano, K.; Nishino, Y.; Yano, S. Macromol Rapid Commun 2000, 21, 396.
- Kim, W.; Bae, J. W.; Choi, D.; Yong, S. K. Polym Eng Sci 1999, 39, 756.
- Kumlatas, D.; Tavman, I. H.; Coban, M. T. Comp Sci Technol 2003, 63, 113.
- Agari, Y.; Ueda, A.; Tanaka, M.; Nagai, S. J Appl Polym Sci 1990, 40, 929.
- Beneviste, Y.; Miloh, T. Int J Eng Sci 1986, 24, 1537.
- Hill, R.; Supancic, P. H. J Am Ceram Soc 2004, 87, 1831.
- Hill, R.; Supancic, P. H. J Am Ceram Soc 2002, 85, 851.
- Holliday, L.; Robinson, L. J Mater Sci 1973, 8, 301.
- Calleja, F. J. B. Trends Polym Sci 1994, 2, 419.